Materials Research, Vol. 12, No. 2, 211-218, 2009

A Study of Al-Mo Powder Processing as a Possible Way to Corrosion Resistent Aluminum-Alloys

Wilson Corrêa Rodrigues[a], *Fidel Romel Mallqui Espinoza*[a],

Lírio Schaeffer[a], *Gerhard Knörnschild*[b]*

[a]*Department of Metallurgy, Laboratory for Metal Forming*
[b]*Department of Metallurgy, Laboratory for Electrochemical Processes and Corrosion,*
Federal University of Rio Grande do Sul – UFRGS,
Av. Bento Gonçalves, 9500, 91501-970 Porto Alegre - RS, Brazil

Received: January 23, 2009; Revised: April 8, 2009

Elementary Al and Mo powder mixtures have been processed by high energy ball milling up to milling times of 100 hours. The shift of the pitting potential and the X ray analysis of green milled samples showed that part of the Mo has formed a supersaturated solid solution of Mo in Al. Elementary Mo powder, however, was still present after 100 hours of milling. Sintering led to the formation of the intermetallic $Al_{12}Mo$ phase.

Keywords: *mechanical alloying, supersaturated alloys, localized corrosion*

1. Introduction

Aluminum alloys are susceptible to pitting corrosion in chloride containing solutions. Massive pitting sets in when a critical potential, the so called pitting potential is reached. Alloying elements can influence this critical potential. However, among the alloying elements contained in technical alloys, only Cu shifts the pitting potential up to about 150 mV to the noble direction, but this is not enough to obtain a substantial improvement of the corrosion resistance. In the nineties researchers produced supersaturated Al alloys, mostly alloyed with transition elements such as Mo, W, Ta, Zr, Nb, Cr, Ni[1-4]. Also rare earth elements have been added more recently[5]. Since the solubility of these elements in Al is very low, they have to be produced by non-equilibrium methods like PVD, ion-implantation or melt-spinning. Electrodeposition from ionic liquids has also been applied for supersaturated aluminum alloys[6]. Shifts of more than 1V were reported for the pitting potential of some alloys in chloride solution[1]. However, the drawback of these materials is that they can be produced only as deposited thin films or as thin ribbons, which does not permit their direct technical use. Although it is known that supersaturated alloys can also be produced by high energy ball milling[7], until now the powder metallurgical way to corrosion resistant supersaturated aluminum alloys has not been examined. Therefore the aim of this paper is to study high energy ball milling, compaction and sintering heat treatment as a possible production way for bulk supersaturated Al-Mo alloys with better resistance to localized corrosion.

Studies about mechanical alloying of aluminum with transition elements are scarce. Zdujic et al.[8] examined the system aluminum – molybdenum. They reported that in their tests a supersaturated solution of molybdenum in aluminum was formed. They chose low velocity (90 rpm.), i.e. low energy, extremely long milling times (up to 1,000 hours) and a high ball: powder weight ratio (90:1) in order to study the alloying process. So far, no information exists about sintering of these materials or about the electrochemical properties of green and of sintered Al-Mo alloys.

*e-mail: gerhard.hans@ufrgs.br

In the present work, two powders of pure Al and of pure Mo, respectively, have been mixed (composition: Al with 15 at.% Mo) and processed by ball milling. The structural changes of the powder vs. milling time were analyzed by X ray diffraction and by scanning electron microscopy up to a milling time of 100 hours. The pitting potentials of the green and of the sintered alloy were determined in NaCl-solution.

2. Experimental Methods

2.1. Materials

The raw materials used in this work were elementary powders of aluminum and of molybdenum. The aluminum powder from Alcoa had a purity of 99.7% and the following particle size distribution: +100#: 0%, +200#: 0.1%, +325#: 11.5%, –325#: 88.4%, according to the manufacturer's analysis. The molybdenum powder from Aldrich had a purity of 99.9+% and an average particle size <10 μm (–100#). The two powders were mixed before milling and 1 wt.(%) of stearic acid was added as process controlling agent.

2.2. Milling process

Milling was performed in a ball mill type Netzsch Molinex PE5. The mill had a stainless steel rotator and chromium steel balls of 6 mm diameter. The ball to powder weight ratio was 10:1. The mill was water cooled and the chamber was purged with argon during the milling process. Milling was carried out with a velocity of 400 rpm. The milling process was interrupted several times in order to remove a small quantity of powder for analysis.

A maximum milling time of 100 hours was considered as convenient. Zdujic et al.[8] reported that after this milling time, with low energy, molybdenum was finely dispersed in the aluminum matrix.

2.3. Compaction and sintering

After milling, the powder was compacted, using a cylindrical matrix and a press which applied a pressure of 400 MPa. The sintering of the compacted powder was carried out in a tubular furnace in an argon atmosphere. The temperature was increased at a rate of 5 °C/min up to 420 °C. The temperature was held at this value for 30 minutes and then raised up to 600 °C at a rate of 5 °C/min. At 600 °C, the specimens were held for 60 minutes.

2.4. X ray analysis

The X ray analyses were performed with a Siemens Kristalloflex 810 diffractometer with a goniometer D500.

2.5. Electrochemical tests

The samples produced with the matrix were cylinders of 12 mm diameter and a height of about 10 mm. For electrical contact a copper wire was connected at the backside with conductive silver glue. Backside and lateral areas of the cylinder were isolated by epoxy resin. The front side, exposed to the electrolyte, had an area of about 1,1 cm^2 and was prepared by grinding up to 1200 grit finish, cleaned with distilled water in an ultrasonic bath and dried in air short time before the tests. The conventional 3-electrode equipment consisted of the working electrode, a Pt-counter electrode and a AgCl/Ag reference electrode. All potentials mentioned in this work refer to the normal hydrogen scale. The corrosion tests with compacted green and with heat treated specimens were performed in an open glass cell at 25 °C in air-saturated 1M NaCl solution. The pitting potentials were measured galvanostatically. Using a PINE-AFCBP1-potentiostat current densities of 0.05, 0.1, 0.5, 1, 5, 10 and 20 mA/cm^2 were applied, beginning with the lowest value. The specimens were held for 8 minutes at each current density. The potential transients were recorded with a PC-based data acquisition system. Some of the specimens were analyzed by scanning electron microscopy after the corrosion tests.

3. Results

3.1. Characterization of the milling process

3.1.1. Scanning electron microscopy

Samples taken from the milling chamber after defined milling times were analyzed by scanning electron microscopy.

The elementary Al powder consisted of elongated particles, typical for powders produced by atomizing (Figure 1a). The size varied between 1 and 100 µm and the surface showed a cellular structure with cell diameters of 1 to 5 µm (Figure 1b). The elementary Mo powder consisted of small crystallites with diameters between 1 and 8 µm. An agglomeration of the Mo particles was observed at the beginning of the milling process (Figure 1c).

The Al powder is heavily deformed after 1 hour of milling and the Mo particles become more and more incorporated into the bigger and softer Al particles (Figure 2b). The particle size grows by cold welding up to a milling time of 70 hours (Figure 2c-e). Particles flattened by plastic deformation prevail after 70 hours (Figure 2e). After 100 hours embrittlement by work hardening caused fracturing of the particles. The particle size has therefore diminished considerably and the particle shape has become more globular (Figure 2f).

During the milling of the powder mixture the distribution of the Mo particles can be monitored by backscattered electron imaging, where the much heavier Mo appears bright due to mass contrast. One observes a constant diminishing of the Mo particle size with longer milling times and the distribution becomes more uniform (Figure 3a-f). However, isolated Mo particles can still be seen after 100 hours of milling (Figure 3f).

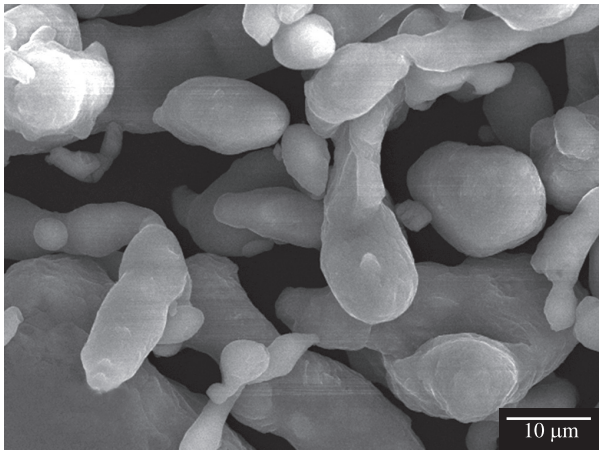

(a)

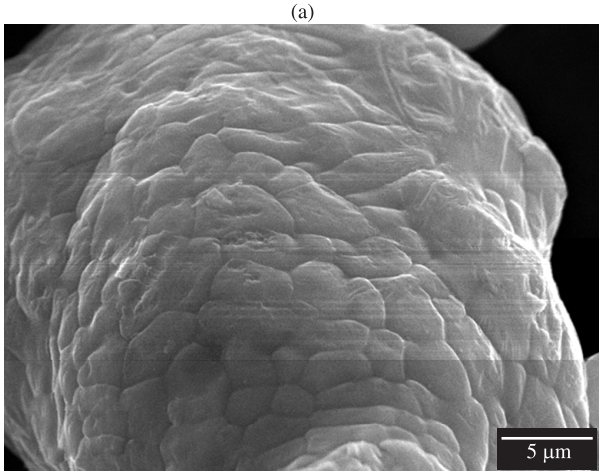

(b)

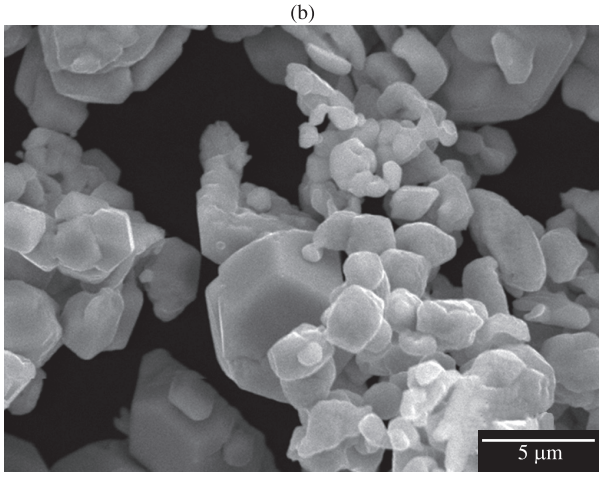

(c)

Figure 1. Raw material: a, b) Al-powder; and c) Mo-powder.

3.1.2. X ray Diffraction

The analysis by X ray diffraction vs. milling time of the powder revealed only elementary Al- and Mo-peaks, i.e., no intermetallic phases have been formed during the milling process (Figure 4). Peak broadening was observed due to diminishing crystallite size

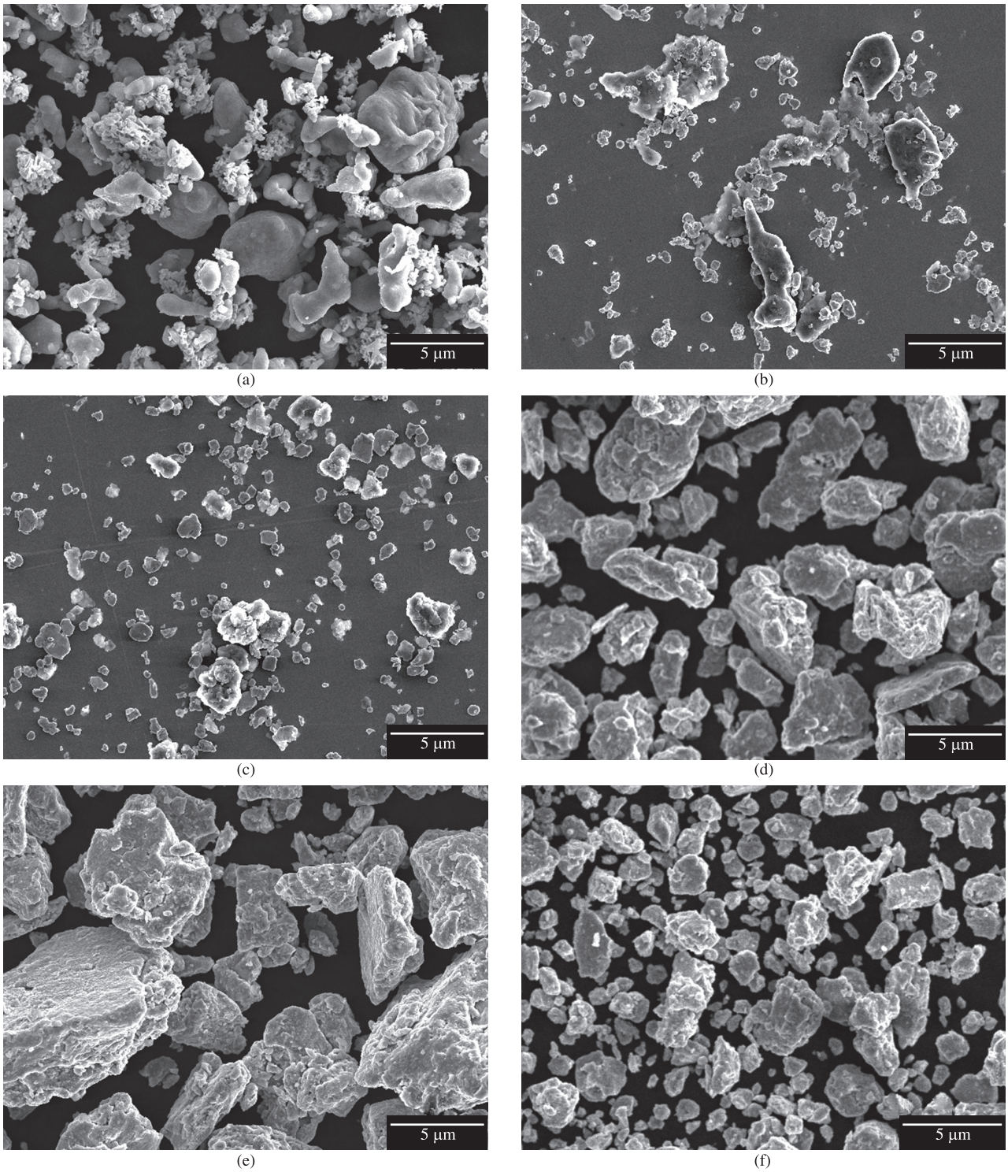

Figure 2. Morphology of Al-Mo powder mixture vs. milling time. Scanning electron micrographs, secondary electron images. Milling time: (a) 0 hours, (b)1 hour, (c) 10 hours, (d) 40 hours, (e) 70 hours, (f) 100 hours.

and straining during the milling process. The crystallite size D was estimated from the broadening of the diffraction peaks, using Scherrer's formula:

$$D = 0.9\lambda \bullet / W \bullet \cdot \cos \Theta \quad (1)$$

with: $\lambda = 0.154060$ nm, W = peak width at half maximum, Θ = peak position.

After 40 hours of milling the calculated values remained nearly constant at about 25 nm for Al crystallites and about 15 nm for Mo crystallites (Figure 5).

A slight shift of the diffraction peaks towards smaller lattice spacing as a function of milling time was observed for Al (Figure 6a). The Mo peaks did not change significantly (Figure 6b).

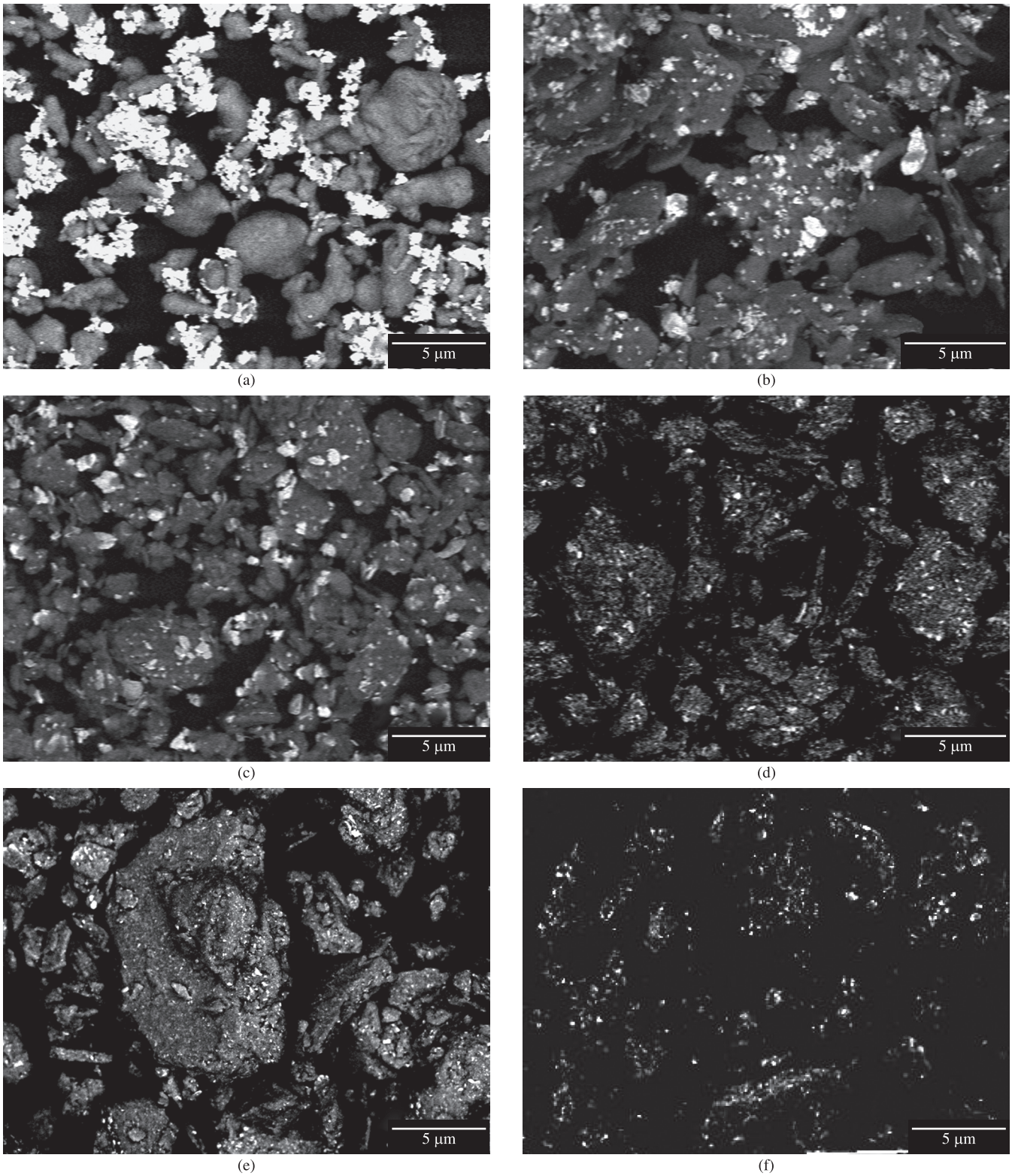

Figure 3. Morphology of Al-Mo powder mixture vs. milling time. Scanning electron micrographs, backscattered electron images. Milling time: (a) 0 hours, (b) 1 hour, (c) 10 hours, (d) 40 hours, (e) 70 hours, (f) 100 hours.

3.2. Electrochemical tests with compacted green alloy

The threshold potential for pitting corrosion was measured galvanostatically with compacted, green specimens in 1 mol.L^{-1} NaCl solution. Within the period of eight minutes in which the samples were held at each current density the potential usually reached a rather stable value. When the current density was increased an anodic "overshot" of the potential was observed, especially at higher applied current densities. Within a few minutes the potential returned from this high anodic value to a rather constant potential (Figure 7). The pitting potential measured with the green alloy sample after 25 hours of mill-

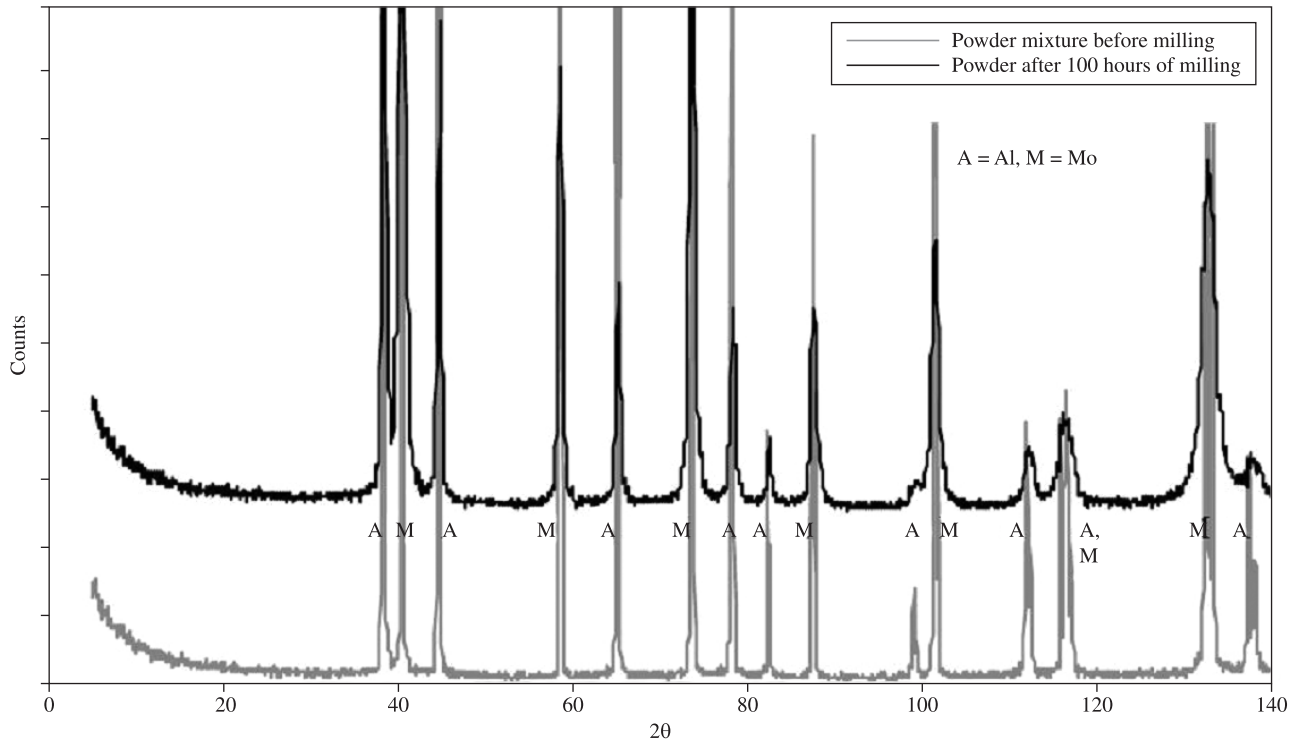

Figure 4. X ray diffraction of the powder mixture vs. milling time.

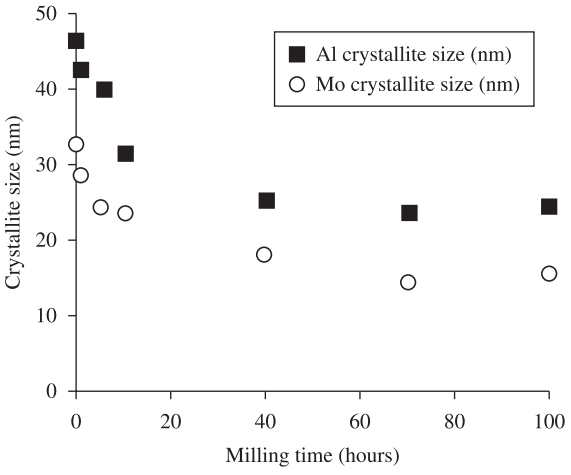

Figure 5. Crystallite size of Mo and Al as a function of milling time, calculated by Scherrer's formula.

ing did not differ significantly from the pitting potential of pure Al. The pitting potential measured with the green sample after 100 hours of milling had a pitting potential about 100 mV higher than the pure Al when low current densities were applied and about 150 mV higher when higher current densities were applied (Figure 7).

3.3. Corrosion attack on the compacted green alloy

The green samples of the supersaturated alloy which showed a shift of the pitting potential were examined by scanning electron microscopy after the corrosion tests. The studies showed how the corrosion attack is correlated with the porosity of the samples.

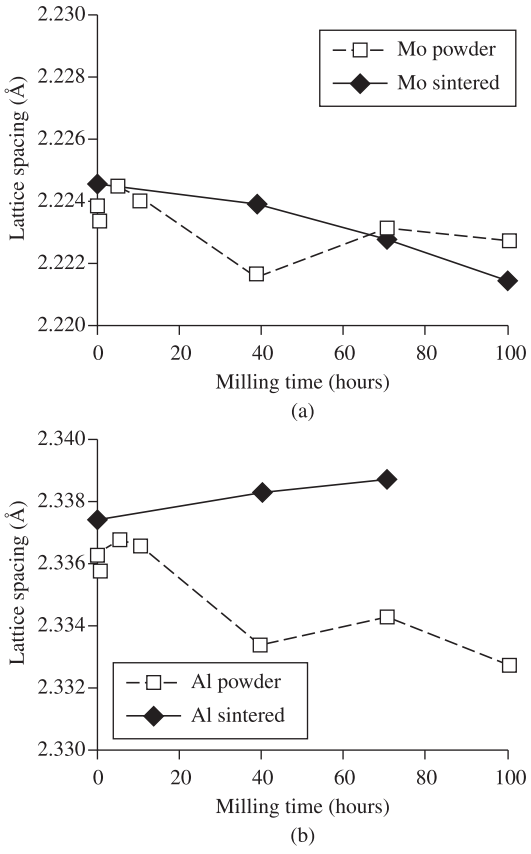

Figure 6. a) Lattice spacing vs. milling time of molybdenum in the powder and in the compacted and sintered specimens; b) lattice spacing vs. milling time of aluminum in the powder and in the compacted and sintered specimens.

The density of samples pressed with powder of 70 hours milling is about 86% of the samples pressed with unmilled powder. The lower density is due to the formation of cold welded, flat particles which grow during the milling process and make compaction more difficult (Figure 8a). Pitting attack on these samples is localized in the pores and crevices between the alloy particles and becomes visible by the thick layers of corrosion products, which form over the pits inside the pores and crevices (Figure 8b). At the samples pressed with powder of 100 hours milling the particle size has diminished, leading to smaller pores (Figure 9a). The pitting attack on these samples is also occluded by corrosion product layers. Now, with smaller pores, the corrosion products accumulate as hillocks on the surface (Figure 9a,b). EDS-analysis showed high aluminum and chlorine concentrations besides oxygen in the corrosion products. The molybdenum concentration, on the other hand, was far below the molybdenum concentration of the alloy, presumably indicating selective dissolution of the alloy. The attacked sites were randomly distributed over the surface. The samples' border wasn't a preferred site for pitting attack.

3.4. Microstructure after sintering

X ray diffraction of the powder mixture, sintered in the as-received condition (i.e. without milling) shows only Al and Mo diffraction peaks (Figure 10). With growing milling times, the Al and Mo peaks become smaller and diffraction peaks of the intermetallic $Al_{12}Mo$ phase are appearing. Up to a milling time of 70 hours, Al and Mo peaks are still present beside the $Al_{12}Mo$ peaks. In the X ray spectrum of specimens sintered after 100 hours of milling, the Al peaks have almost completely disappeared, remaining only the intermetallic $Al_{12}Mo$ phase and some small peaks of metallic Mo (Figure 10). The Al peaks, which were shifted towards smaller lattice spacing during milling, returned after sintering to a peak position close to that of the as-received Al-powder (Figure 6b).

3.5. Electrochemical behavior after sintering

For short milling times the electrochemical behavior of the heat treated alloy is determined by the presence of Al particles. The pitting potential is close to the value of pure aluminum in 1M chloride solution, which is in agreement with the X ray analysis. With the proceeding of milling it becomes slightly more negative as the particle size diminishes (Figure 11). Obviously, with heterogeneities at a smaller scale and an increase of the number of interfaces pit initiation is facilitated. The electrode behavior changes significantly after 70 hours of milling (Figure 12). The Al has been consumed almost completely by the formation of $Al_{12}Mo$. Although the X ray spectrum still demonstrates the presence of some Al, these particles seem to be so small that they do not permit the formation of pits which sustain an elevated current density. The pitting potential of around +100 mV(NHE) of the samples after 70 hours and 100 hours of milling seems to reflect the behavior of the $Al_{12}Mo$ phase, since for pure molybdenum in 1M chloride solution the literature reports a significantly higher value of +650 mV(NHE)[9].

4. Discussion

X ray diffraction of the Al-Mo powder mixture showed slightly lower lattice spacing with growing milling times. This is the expected result in the case of the formation of a supersaturated substitutional solid solution of Al-Mo. It agrees with the results reported by Zdujic et al.[8]. As in the present work, elementary Mo was still present after milling. Zdujic estimated that 2.4 at.% were homogeneously dissolved in Al in an Al-17 at.% Mo powder mixture. The homogeneously dissolved Mo in the powder mixture of the present work can

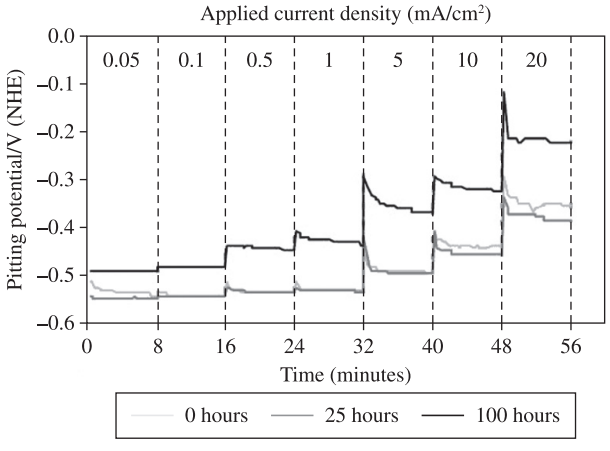

Figure 7. Pitting potential of compacted green Al-15at.%Mo powder, measured galvanostatically in 1M NaCl solution.

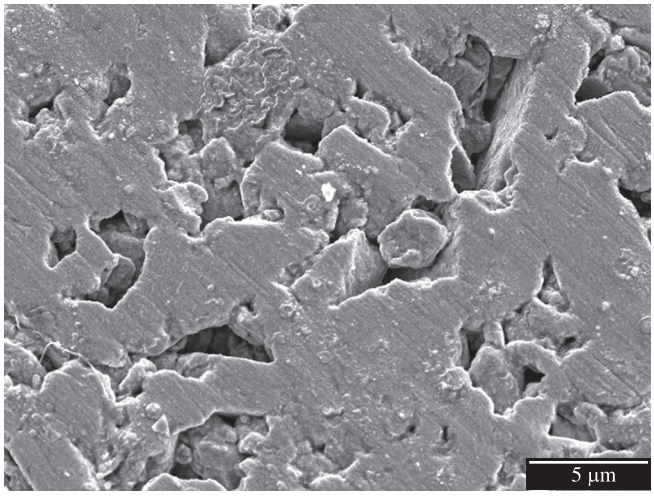

(a)

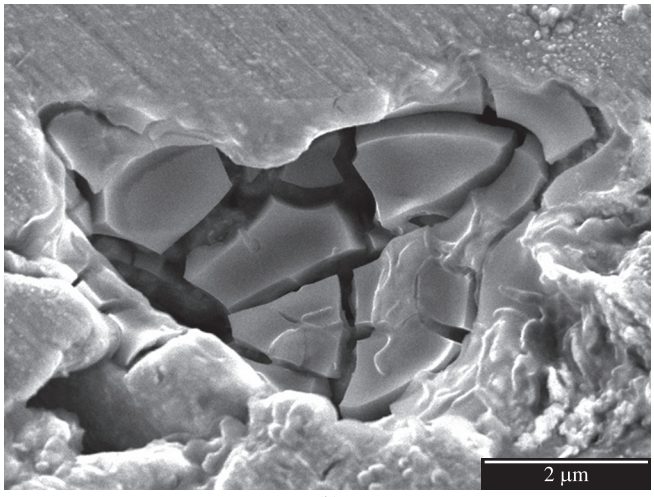

(b)

Figure 8. a) Surface of sample with powder of 70 hours milling time before corrosion test; b) surface of sample with powder of 70 hours milling time after corrosion test in 1M NaCl solution.

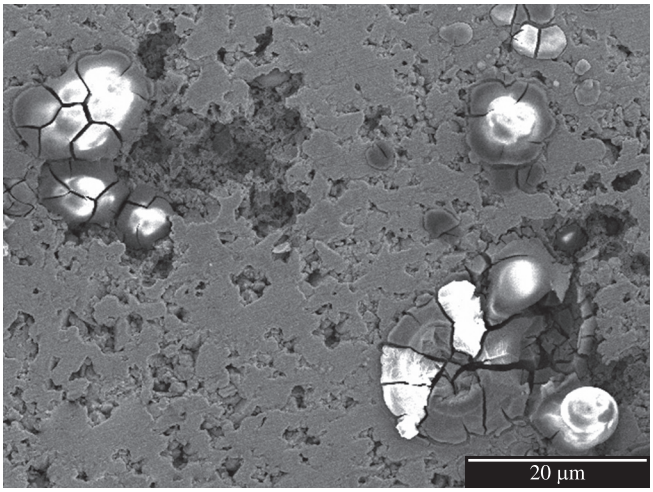

(a)

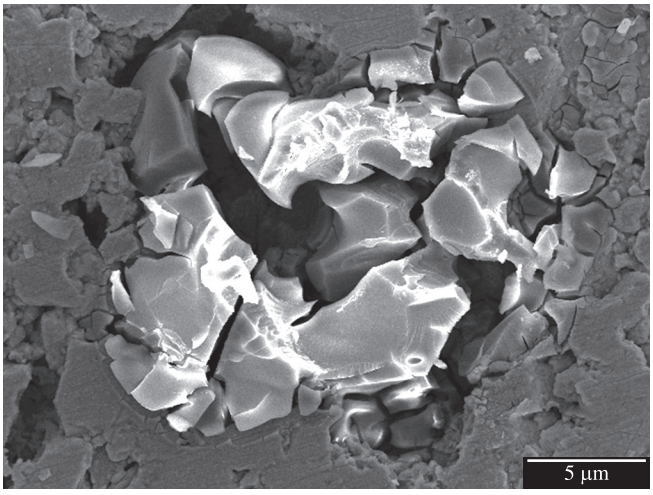

(b)

Figure 9. a) Overview of pitting attack on sample with powder of 100 hours milling time; and b) pit on sample with powder of 100 hours milling time.

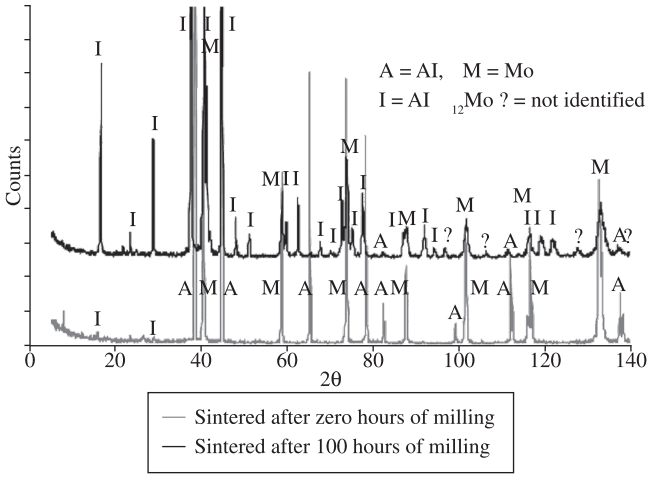

Figure 10. X ray diffraction of sintered specimens as a function of the milling time.

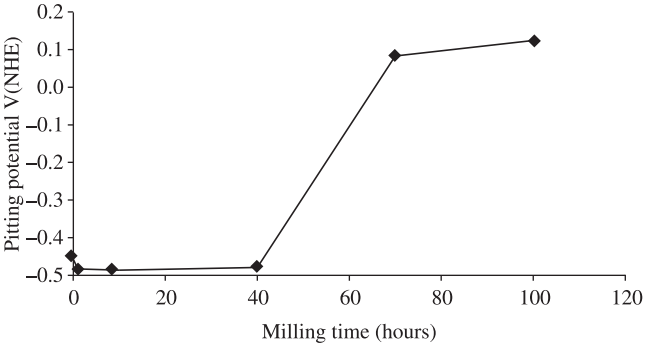

Figure 11. Pitting potential in 1M NaCl of sintered Al-15 at.Mo alloy vs. milling time.

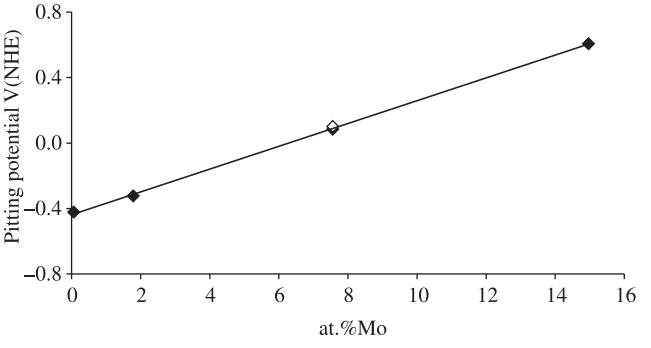

Figure 12. Pitting potential in 1M NaCl of: ◆ Al-Mo PVD-alloys[10] and of: ◇ $Al_{12}Mo$ phase (7.7 at.%Mo).

be estimated by a comparison with data from Al-Mo alloys produced by PVD[10] (Figure 12). The shift of the pitting potential of 100 mV to 150 mV towards the noble direction points to a Mo content between 1 at.% and 2 at.% in solid solution. It can be discussed if other structural changes introduced by the milling process have an influence on this result. Sweitzer et al.[5] mentioned that amorphization tends to elevate the pitting potential since it eliminates microstructural elements such as grain boundaries and interface boundaries which represent typical sites for pit initiation. The shift of the pitting potential of the green alloy in the present work occurs despite of the presence of finely distributed Mo particles. This points to solid solution formation as the main reason for pitting potential shift.

The negative influence of fine scaled inhomogeneities was confirmed in the case of the heat treated alloy, which showed after short milling times a pitting potential slightly more negative than pure Al. The same observation was made by Sweitzer et al.[5] in the case of the pitting potential of a heat treated Al-Fe-Gd alloy due to the presence of finely distributed precipitates.

Research about amorphous alloys generally does not include examination of the pitting morphology since there is no correlation with microstructural features of the alloys. Nevertheless microscopic characteristics such as pits with irregular borders or hemispherical pits with electropolished smooth surfaces might give some information about the mechanism of pit growth. However, in the present work the preferential formation of pits in pores and crevices and the formation of thick product layers over the pits impeded such observations.

Mechanical compaction and heat treatment are the necessary steps to obtain bulk material with a sufficient resistance and close to the theoretical density. It is clear that the heat treatment step is the most critical, when the purpose is the maintenance of the supersaturated microstruture produced during milling. The treatment applied in the present work was not able to maintain this microstructure and thus the better corrosion resistance of the green alloy. However there might

be alternative procedures which permit a better preservation of the corrosion resistant microstructure.

The possibility of cold sintering, powder consolidation at high pressures up to 3 GPa and heat treatment at rather low temperatures has been described by Gutmanas[11].

Sweitzer et al.[5] have reported that the corrosion resistance of supersaturated AlFeGd and AlNiY alloys can be maintained after a heat treatment of 25 hours at 150 °C. During this treatment nanocrystals of 15 nm size have been formed, embedded in an amorphous matrix. This nanocrystal formation has been observed up to 400 °C. Only above this temperature the mechanism is substituted by direct formation of precipitation phases.

In the case of Al-Cu alloys it has been observed that the formation of Cu-clusters (GP-zones) does not alter the pitting potential of a homogeneous Al-1.7at.%Cu alloy[12].

These examples show that diffusion processes occurring during sintering do not necessarily destroy completely the corrosion resistant microstructure. Only the formation of equilibrium phases in systems with low solubility of the solute elements must be avoided.

Spark plasma sintering might be another promising technique, which permits sintering at lower temperatures. Recently the ability of producing ultrahigh strength bulk Al-based amorphous/nanocrystalline composites with the aid of spark plasma sintering was shown by Sasaki[13].

The sintered alloy with 100 hours of milling showed an interesting electrochemical behavior, since the matrix is free of Al and the behavior is determined by the elevated pitting potential of the $Al_{12}Mo$ phase. Figure 10 shows that the pitting potential of about +0.1V is consistent with the value expected for a homogeneous alloy with 7.7 at.% Mo (equivalent with the Mo content of the $Al_{12}Mo$ phase), assuming a linear influence of Mo on the pitting potential. However, since the present work is focused on supersaturated alloys, the mechanical properties and the application potentialities of this material was not further examined.

5. Conclusions

The tests proved that supersaturated Al-Mo alloys with enhanced resistance to localized corrosion can be made by high energy milling of elementary Al and Mo powders. A shift of the pitting potential of 100-150 mV was obtained with compacted powder after 100 hours of milling, indicating the formation of a supersaturated alloy with 1-2at.% Mo in solid solution. The production of supersaturated powder can be seen as first step to obtain stainless bulk material. However the milling process has to be improved in order to increase the Mo content in solid solution and thus further increase the pitting potential of the alloy. Alternative consolidation treatments such as cold sintering or spark plasma sintering might be tried in order to preserve the corrosion resistant microstructure developed by high energy ball milling.

References

1. Shaw BA, Davis GD, Fritz TL, Rees RJ, Moshier WC. The influence of Tungsten alloying additions on the passivity of Aluminum. *Journal of the Electrochemical Society.* 1991; 138(11):3288-3295.
2. Davis GD, Moshier WC, Fritz TL, Cote GO. Surface-chemistry of sputter-deposited Al-Mo and Al-Cr alloys polarized in 0.1N KCl. *Journal of the Electrochemical Society.* 1989; 136(2):356-362.
3. Natishan PM, McCafferty E, Hubler GK. Surface charge considerations of ion-implanted aluminum. *Journal of the Electrochemical Society.* 1988; 135(2):321-327.
4. Davis GD, Moshier WC, Long GG, Black DR. Passive film structure of supersaturated Al-Mo alloys. *Journal of the Electrochemical Society.* 1991; 138(11):3194-3199.
5. Sweitzer JE, Shiflet GJ, Scully JR. Localized corrosion of Al90Fe5Gd5 and Al87Ni8.7Y4.3 alloys in the amorphous, nanocrystalline and crystalline states: resistance to micrometer-scale pit formation. *Electrochimica Acta.* 2003; 48(9):1223-1234.
6. Tsuda T, Arimoto S, Kuwabata S, Hussey CL. Electrodeposition of Al-Mo-Ti ternary alloys in the Lewis acidic aluminum chloride-1-ethyl-3-methylimidazolium chloride room-temperature ionic liquid. *Journal of the Electrochemical Society.* 2008; 155(4):D256-D262.
7. Uenishi K, Kobayashi KF, Ishihara KN, Shingu PH. Formation of supersaturated solid solution in Ag-Cu system by mechanical alloying. *Materials Science and Engineering.* 1991; A134:1342-1345.
8. Zdujic MV, Kobayashi KF, Shingu PH. Structural changes during mechanical alloying of elemental aluminium and molybdenum powders. *Journal of Materials Science.* 1991; 26(20):5502-5508.
9. Metikoš-Huković M, Babić R. Some aspects in designing passive alloys with an enhanced corrosion resistance. *Corrosion Science.* 2009; 51(1):70-75.
10. Atz NR, Knörnschild G, Dick LFP. Corrosão localizada de ligas Al-Mo produzidas por PVD. In: XIII Congresso de la Sociedad Iberoamericana de Eletroquimica; 1998; Vinã del Mar, Chile. Vinã del Mar: Editora Sociedad Iberoamericana deElectroquímica; 1998. p. 393.
11. Gutmanas EY. New materials by mechanical alloying techniques. In: *DGM Conference "New Materials by Mechanical Alloying Techniques"*; 1988; Calw-Hirsau. Germany: Editora Deutsche Gesellschaft für Metallkunde; 1988. p.129-142.
12. Knörnschild G, Kaesche H. Pitting morphology and tunnel propagation in homogeneous binary Al-Zn and Al-Cu alloys. In: Frankel GS, Watson TJ, Newman RC. (Eds.). *Proceedings of the Symposium on Critical Factors in Localized Corrosion*. New Jersey: Pennington; 1992. p. 266-267.
13. Sasaki TT, Hono K, Vierke J, Wollgarten M, Banhart J. Bulk nanocrystalline Al85Ni10La5 alloy fabricated by spark plasma sintering of atomized amorphous powders. *Materials Science and Engineering A.* 2008; 490(1-2):343-350.